

Right-handed current with CP violation in the $b \rightarrow u$ transition

Tetsuya ENOMOTO* and Minoru TANAKA†

Department of Physics, Graduate School of Science,

Osaka University, Toyonaka, Osaka 560-0043, Japan

Abstract

We show that the experimental data on $|V_{ub}|$ in various B meson decay modes suggest a possibility of CP -violating right-handed current in the $b \rightarrow u$ transition. Its consequences in $B \rightarrow \pi\pi$, $\rho\rho$, DK are examined and compared with experimental results in order to clarify possible signals of the CP violation in these decay modes. As a result, we find that the CP -violating right-handed current is consistent with current experimental data. Its signal might be discovered by precise CP measurements in future experiments.

PACS numbers: 13.20.He, 13.25.Hw, 11.30.Er

arXiv:1411.1177v2 [hep-ph] 9 Nov 2014

* tetsuya@het.phys.sci.osaka-u.ac.jp

† tanaka@phys.sci.osaka-u.ac.jp

I. INTRODUCTION

Left-handedness is the most interesting nature of the weak charged current. The charged weak boson W couples only to the left-handed fermions in the standard model (SM), and this structure of the SM results in purely left-handed charged currents. Another notable aspect of the weak charged current is the Cabibbo-Kobayashi-Maskawa (CKM) mixing in the quark sector [1, 2]. Because of the CKM mixing the strength of the quark charged current varies depending on the flavors involved in a transition, while the left-handedness remains universal apart from tiny radiative corrections.

New physics (NP) beyond the SM may violate the universality of the charged current. In particular, NP effects are expected to be significant for CKM suppressed transitions if the supposed NP has a different flavor structure from the SM. Among several CKM suppressed channels, the $b \rightarrow u$ transition is most likely to be affected by NP in this sense. Moreover, we can examine it with the competent data of B factory experiments.

It was pointed out that a mixture of right-handed current (RHC) in the $b \rightarrow u$ charged current explained the discrepancy among magnitudes of the relevant CKM matrix element, $|V_{ub}|$, determined by various B decay modes [3–5]. Recently, Belle collaboration updated the data on the pure tauonic B decay, $B^- \rightarrow \tau \bar{\nu}$ ¹ [6], and the new result seems more consistent with the SM than the previous one [7].

In this work, we revisit the possibility of RHC in the $b \rightarrow u$ transition taking the new Belle data into account. In Sec. II, we introduce the $b \rightarrow u$ RHC and explain how it affects the $|V_{ub}|$ determination in leptonic and semileptonic B decays. Then, we show that the present experimental data suggest a sizable CP -violating (CPV) RHC in this transition. According to this observation, we study possible CPV signals in hadronic B decays, $B \rightarrow \pi\pi$, $B \rightarrow \rho\rho$ and $B \rightarrow DK$, in the presence of the $b \rightarrow u$ RHC in Sec. III. We find that new CPV signals absent in the SM arise in direct CP asymmetries and the measurement of angles of the unitarity triangle. Comparing these possible signals of the RHC with the relevant experimental data, we show that the $b \rightarrow u$ CPV RHC is a viable NP scenario. We also compare the $b \rightarrow u$ RHC induced by squark mixings in the minimal supersymmetric standard model (MSSM) to the experimental constraint obtained in Sec. II. Our conclusion is given in Sec. IV.

¹ Charge-conjugation modes are implied unless otherwise stated.

II. EFFECTS OF THE RIGHT-HANDED CURRENT IN $|V_{ub}|$ DETERMINATION

A set of right-handed quark charged currents appears in the SM once we introduce higher dimensional operators. The gauge-invariant effective lagrangian containing the lowest dimensional operator responsible for the $b \rightarrow u$ transition is expressed by

$$\mathcal{L}_R = \frac{C_R}{\Lambda^2} \tilde{\phi}^\dagger i D_\mu \phi \bar{u}_R \gamma^\mu b_R + \text{h.c.}, \quad (1)$$

where ϕ is the Higgs doublet, $\tilde{\phi} = i\sigma_2 \phi^*$, Λ represents the energy scale of NP, and C_R is a dimensionless constant that depends on the details of NP. This lagrangian leads to the desired right-handed interaction as a result of the electroweak symmetry breaking.

Combined with the ordinary left-handed interaction, the $b \rightarrow u$ transition is described by the following modified charged current lagrangian:

$$\mathcal{L}_{CC} = -\frac{g}{\sqrt{2}} \bar{u} \gamma^\mu (V_{ub}^L P_L + V_{ub}^R P_R) b W_\mu^+ + \text{h.c.}, \quad (2)$$

where g is the SU(2) gauge coupling, $P_{L(R)} = (1 \mp \gamma_5)/2$, and V_{ub}^L denotes the left-handed CKM matrix element. The effective right-handed CKM matrix element V_{ub}^R is given by

$$V_{ub}^R = C_R v^2 / 2\Lambda^2 \sim 3 \times 10^{-3} C_R \left(\frac{3 \text{ TeV}}{\Lambda} \right)^2, \quad (3)$$

where $v \simeq 246$ GeV denotes the vacuum expectation value of ϕ . The known magnitude of the $b \rightarrow u$ charged current corresponds to $|V_{ub}^L| \sim 3.6 \times 10^{-3}$ and the right-handed component induced by NP at the TeV scale is potentially comparable.

In the rest of this section, we treat V_{ub}^L and V_{ub}^R as complex parameters and determine their values using experimental data of leptonic and semileptonic B meson decay modes along with the unitarity of the left-handed CKM matrix V^L assuming that no SM interactions besides the RHC in Eq. (2) are affected by NP. We emphasize that the nonvanishing relative phase between V_{ub}^L and V_{ub}^R is a new CPV degree of freedom.

A. $B \rightarrow \tau \bar{\nu}$

The pure tauonic B decay is a theoretically clean mode to determine $|V_{ub}|$ provided that the B meson decay constant f_B is known accurately enough. The decay rate is written as

$$\Gamma(B^- \rightarrow \tau^- \bar{\nu}) = \frac{G_F^2 m_B m_\tau^2}{8\pi} \left(1 - \frac{m_\tau^2}{m_B^2} \right) f_B^2 |V_{ub}^{\text{exp}}|^2, \quad (4)$$

where $|V_{ub}^{\text{exp}}|$ is the effective CKM matrix element that is determined by experiments assuming the SM. Since the axial-vector current contributes to this decay mode, one finds $|V_{ub}^{\text{exp}}| = |V_{ub}^L - V_{ub}^R|$ in the presence of the RHC in Eq. (2).

The present world average of the branching ratio including the updated Belle data is provided by the heavy flavor averaging group (HFAG) [8] as $\text{Br}(B \rightarrow \tau \bar{\nu}) = (1.14 \pm 0.22) \times 10^{-4}$. Using this value and $f_B = 190.5 \pm 4.2$ MeV [9], we obtain

$$|V_{ub}^{\text{exp}}| = |V_{ub}^L - V_{ub}^R| = (4.22 \pm 0.42) \times 10^{-3}. \quad (5)$$

B. $B \rightarrow \pi \ell \bar{\nu}$

The axial-vector part in Eq. (2) does not contribute to the process $B \rightarrow \pi \ell \bar{\nu}$ owing to the parity invariance of the strong interaction. The contribution of the vector part leads to the following differential decay rate,

$$\frac{d\Gamma}{dq^2} = \frac{G_F^2}{192\pi^2 m_B^3} \lambda^{3/2}(q^2) f_+^2(q^2) |V_{ub}^{\text{exp}}|^2, \quad (6)$$

where q^μ represents the momentum transfer, $\lambda(q^2) = q^4 - 2q^2(m_B^2 + m_\pi^2) + (m_B^2 - m_\pi^2)^2$, and $|V_{ub}^{\text{exp}}| = |V_{ub}^L + V_{ub}^R|$, which reduces to the ordinary CKM matrix element in the absence of the right-handed interaction. The hadronic form factor $f_+(q^2)$ plays a crucial role in the determination of $|V_{ub}^{\text{exp}}|$. We employ the one evaluated using the light-cone sum rule (LCSR) [10] and its explicit form is given in Appendix A 1 for completeness. The mass of the charged lepton is neglected in Eq. (6).

Evaluating the branching ratio with Eqs. (6) and (A2), and comparing it to the experimental result [8], $\text{Br}(B \rightarrow \pi \ell \bar{\nu}, 0 < q^2 < 16 \text{ GeV}^2) = (1.06 \pm 0.04) \times 10^{-4}$, we obtain

$$|V_{ub}^{\text{exp}}| = |V_{ub}^L + V_{ub}^R| = (3.58 \pm 0.47) \times 10^{-3}, \quad (7)$$

where the error includes 13% theoretical uncertainty in the magnitude of $f_+(q^2)$ [10] as well as the experimental errors.

C. $B \rightarrow (\rho, \omega) \ell \bar{\nu}$

Both the vector and axial vector currents give rise to the decay $B \rightarrow V \ell \bar{\nu}$, where V denotes a vector meson and we consider two modes with $V = \rho, \omega$. The differential decay

rate is given as

$$\frac{d\Gamma}{dq^2} = \frac{G_F^2 |\mathbf{p}_V| q^2}{96\pi^3 c_V^2 m_B^2} \sum_{\lambda=\pm,0} |H_\lambda|^2, \quad (8)$$

where \mathbf{p}_V represents the three momentum of the vector meson in the rest frame of the B meson, $c_V = \sqrt{2}$ for $V = \rho^0, \omega$ considered below, and the helicity amplitudes $H_{\pm,0}$ are expressed in terms of hadronic form factors $V(q^2)$ and $A_{1,2}(q^2)$:

$$H_\pm = (V_{ub}^L - V_{ub}^R)(m_B + m_V)A_1(q^2) \mp (V_{ub}^L + V_{ub}^R) \frac{2m_B |\mathbf{p}_V|}{m_B + m_V} V(q^2), \quad (9)$$

$$H_0 = (V_{ub}^L - V_{ub}^R) \frac{m_B + m_V}{2m_V \sqrt{q^2}} \left\{ (m_B^2 - m_V^2 - q^2)A_1(q^2) - \frac{4m_B^2 |\mathbf{p}_V|^2}{(m_B + m_V)^2} A_2(q^2) \right\}. \quad (10)$$

We use LCSR form factors [11] and they are explicitly given in Appendix A 2.

We can experimentally determine the magnitude of the $b \rightarrow u$ charged current, represented by $|V_{ub}^{\text{exp}}|$, from the branching ratio of $B \rightarrow V \ell \bar{\nu}$. Integrating the differential rate in Eq. (8) over the phase space, we find

$$|V_{ub}^{\text{exp}}| = |V_{ub}^L| \sqrt{1 + a_V \text{Re} \left(\frac{V_{ub}^R}{V_{ub}^L} \right) + \left| \frac{V_{ub}^R}{V_{ub}^L} \right|^2}, \quad (11)$$

where $a_V = -1.18(-1.25)$ for $V = \rho(\omega)$. In our numerical analysis, we employ the following experimental results [12]:

$$|V_{ub}^{\text{exp}}| = (3.56 \pm 0.48) \times 10^{-3}, \quad (12)$$

for $B \rightarrow \rho^0 \ell \bar{\nu}$ and

$$|V_{ub}^{\text{exp}}| = (3.08 \pm 0.49) \times 10^{-3}, \quad (13)$$

for $B \rightarrow \omega \ell \bar{\nu}$, where the errors include theoretical uncertainties in the form factors. Since significant part of theoretical uncertainties is involved in these errors, neither the theoretical uncertainty in a_V nor the effect of experimental cut in the phase space integration performed to obtain Eq. (11) is taken into account in the present analysis. We note that a precise study of decay distribution in these modes with copious data at the SuperKEKB/Belle II experiment may provide an improved method to probe the RHC [13].

D. $B \rightarrow X_u \ell \bar{\nu}$

Both the left- and right- handed currents contribute to the inclusive $b \rightarrow u$ semileptonic process. However the interference between them is strongly suppressed because of the small

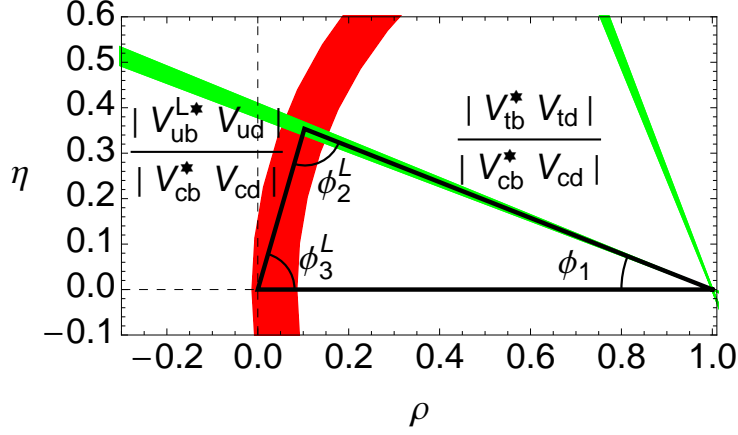


FIG. 1. Unitarity triangle (solid lines). Experimental constraints from the $B-\bar{B}$ mixings and CP violation in $b \rightarrow c\bar{c}s$ decays are also indicated by the red arc and the green narrow sectors respectively.

mass of the up quark. Thus, the decay rate is proportional to $|V_{ub}^{\text{exp}}|^2 = |V_{ub}^L|^2 + |V_{ub}^R|^2$. In our numerical analysis, we use the following result of GGOU method [14] given by HFAG [8]:

$$|V_{ub}^{\text{exp}}| = \sqrt{|V_{ub}^L|^2 + |V_{ub}^R|^2} = (4.39 \pm 0.31) \times 10^{-3}, \quad (14)$$

where the statistic and systematic errors are linearly added in order to take the sizable method dependence into account.

E. Unitarity triangle

Since the above five processes of direct $|V_{ub}|$ measurement are described by two independent quantities, $|V_{ub}^L|^2 + |V_{ub}^R|^2$ and $\text{Re}(V_{ub}^L V_{ub}^{R*})$, they are insufficient to determine the absolute values of V_{ub}^L and V_{ub}^R , and their relative phase. In order to extract more information on V_{ub}^L and V_{ub}^R , we utilize the unitarity of the CKM matrix V^L assuming the validity of the SM except for the V_{ub}^R term in Eq. (2) as stated previously.

The unitarity of V^L is conveniently represented by the unitarity triangle in Fig. 1, where Wolfenstein parameterization [15, 16] is introduced. Measuring $|V_{td} V_{tb}^*|$ by the $B-\bar{B}$ mixings and ϕ_1 (or β) with CP violation in $b \rightarrow c\bar{c}s$ decays, together with results of kaon and $b \rightarrow c$ semileptonic decays that give λ and A in Wolfenstein parameterization, we can indirectly determine the magnitude and phase of V_{ub}^L .

The mass difference in the B_d meson system due to the B_d - \bar{B}_d mixing, denoted by Δm_{B_d} , is dominated by the top quark loop in the SM and proportional to $|V_{td}V_{tb}^*|^2$; and similarly in the B_s system, $\Delta m_{B_s} \propto |V_{ts}V_{tb}^*|^2$. Theoretical uncertainties of the relevant hadronic matrix elements are reduced by taking the ratio of Δm_{B_d} and Δm_{B_s} owing to the SU(3) flavor symmetry:

$$\frac{\Delta m_{B_d}}{\Delta m_{B_s}} = \frac{m_{B_d}}{m_{B_s}} \xi^{-2} \left| \frac{V_{td}V_{tb}^*}{V_{ts}V_{tb}^*} \right|^2 = \frac{m_{B_d}}{m_{B_s}} \xi^{-2} \lambda^2 \{ (1 - \rho)^2 + \eta^2 \}, \quad (15)$$

where $\xi = 1.268 \pm 0.063$ [9] represents the SU(3) breaking effect. Thus, we determine $|V_{td}V_{tb}^*|$ from the present experimental data, $\Delta m_{B_d} = 0.510 \pm 0.003 \text{ ps}^{-1}$ and $\Delta m_{B_s} = 17.761 \pm 0.022 \text{ ps}^{-1}$ [8]. The result is shown as the red arc in Fig. 1.

The time-dependent CP asymmetries in $b \rightarrow c\bar{c}s$ processes such as $B \rightarrow J/\psi K_S$ give $\sin 2\phi_1$ with small theoretical uncertainty in the SM. This argument does not change in the presence of the $b \rightarrow u$ RHC. The combined experimental data $\sin 2\phi_1 = 0.682 \pm 0.019$ [8] gives ϕ_1 with a four-fold ambiguity. It turns out that only the solution favored in the SM, as depicted in Fig. 1, is consistent with the RHC.

Consequently, one of the apices of the unitarity triangle (ρ, η) is uniquely determined (with errors) and $V_{ub}^L = \lambda^3 A(\rho - i\eta)$ is evaluated as

$$|V_{ub}^L| = (3.43 \pm 0.16) \times 10^{-3}, \quad \phi_3^L = \arg V_{ub}^{L*} = 73.8^\circ \pm 7.5^\circ, \quad (16)$$

where $\lambda = 0.225$ and $A = 0.823$ are used [17].

F. Combined result

Combining the results in Eqs. (5), (7), (11), (12), (13), (14) and (16), we obtain a constraint on V_{ub}^R . The numerical result is presented in Fig. 2, where 1σ , 2σ and 3σ allowed regions are indicated by solid lines. The best fit is given by

$$\text{Re} \left(\frac{V_{ub}^R}{V_{ub}^L} \right) = -4.21 \times 10^{-3}, \quad \left| \text{Im} \left(\frac{V_{ub}^R}{V_{ub}^L} \right) \right| = 0.551, \quad |V_{ub}^L| = 3.43 \times 10^{-3}, \quad (17)$$

with $\chi_{\min}^2/\text{dof} = 2.27$. We obtain $\chi_{\min}^2/\text{dof} = 2.16$ in the SM and thus the scenario of the $b \rightarrow u$ RHC exhibits a similar consistency as the SM among the above experimental results in $|V_{ub}|$ determination.

As seen in Fig. 2 and Eq. (17), a large relative phase between V_{ub}^R and V_{ub}^L is favored. We examine its implication for CP violations in hadronic B decays in the next section.

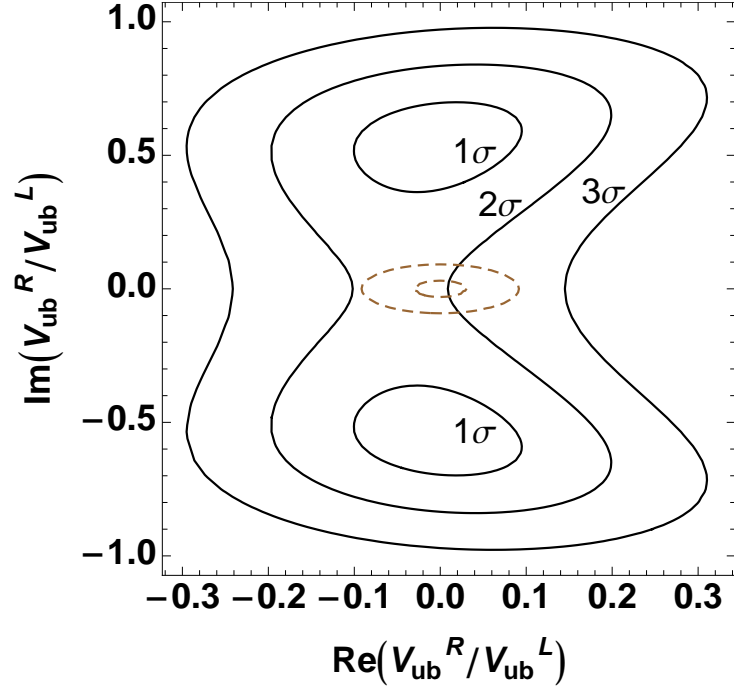


FIG. 2. Allowed region of V_{ub}^R/V_{ub}^L (solid lines). The constraints from $|V_{ub}|$ and the unitarity triangle are combined. Prediction of MSSM is also indicated by dashed lines. (See Sec. IIID.)

III. CP VIOLATIONS INDUCED BY THE $b \rightarrow u$ RIGHT-HANDED CURRENT

As shown in the previous section, the present experimental data related to the $b \rightarrow u$ transition allow the right-handed $b \rightarrow u$ current with a large relative phase to the left-handed counter part. We examine possible consequences of this new complex phase in CP violations in hadronic B decays.

A. $B \rightarrow \pi\pi$

The time-dependent CP asymmetry in $B \rightarrow \pi^+\pi^-$ is described by the following formula [18],

$$A_{\pi^+\pi^-}(t) = C_{\pi^+\pi^-} \cos(\Delta m_{B_d} t) - S_{\pi^+\pi^-} \sin(\Delta m_{B_d} t), \quad (18)$$

where the direct CP asymmetry $C_{\pi^+\pi^-}$ and the mixing-induced CP asymmetry $S_{\pi^+\pi^-}$ are expressed as

$$C_{\pi^+\pi^-} = \frac{1 - |\bar{\rho}(\pi^+\pi^-)|^2}{1 + |\bar{\rho}(\pi^+\pi^-)|^2}, \quad (19)$$

and

$$S_{\pi^+\pi^-} = \frac{2\text{Im}((q/p)\bar{\rho}(\pi^+\pi^-))}{1 + |\bar{\rho}(\pi^+\pi^-)|^2}, \quad (20)$$

respectively. The amplitude ratio $\bar{\rho}(\pi^+\pi^-)$ is defined by

$$\bar{\rho}(\pi^+\pi^-) = \frac{A(\bar{B}^0 \rightarrow \pi^+\pi^-)}{A(B^0 \rightarrow \pi^+\pi^-)}, \quad (21)$$

and the ratio of the B - \bar{B} mixing coefficients is given as $q/p = V_{td}^L V_{tb}^{L*}/V_{td}^{L*} V_{tb}^L$ for the B_d case under consideration here.

The isospin analysis is mandatory to extract the information on the weak phase in this process because of the penguin pollution [19]. The decay amplitudes of the isospin doublet (B^+, B^0) are expressed in terms of the isospin amplitudes $A_I = \langle(\pi\pi)_I|B^0\rangle$ ($I = 0, 2$):

$$A(B^+ \rightarrow \pi^+\pi^0) = \sqrt{\frac{3}{2}}A_2, \quad (22)$$

$$A(B^0 \rightarrow \pi^+\pi^-) = \frac{1}{\sqrt{3}}A_2 + \sqrt{\frac{2}{3}}A_0, \quad (23)$$

$$A(B^0 \rightarrow \pi^0\pi^0) = \sqrt{\frac{2}{3}}A_2 - \frac{1}{\sqrt{3}}A_0. \quad (24)$$

We note a simple triangle relation, $A(B^+ \rightarrow \pi^+\pi^0) = A(B^0 \rightarrow \pi^+\pi^-)/\sqrt{2} + A(B^0 \rightarrow \pi^0\pi^0)$. The (\bar{B}^0, B^-) decay amplitudes bear similar relations to $\bar{A}_I = \langle(\pi\pi)_I|\bar{B}^0\rangle$. The relative phase between A_0 and A_2 can be determined with a twofold ambiguity as well as their magnitudes by measuring the branching fractions of three decay modes in Eqs. (22), (23) and (24); and likewise for (\bar{B}^0, B^-) and \bar{A}_I .

The ratio of $B \rightarrow \pi^+\pi^-$ amplitudes in Eq. (21) is expressed in terms of the isospin amplitudes as

$$\bar{\rho}(\pi^+\pi^-) = \frac{\bar{A}_2}{A_2} \frac{1 + \bar{z}}{1 + z}, \quad (25)$$

where $z = \sqrt{2}A_0/A_2$, $\bar{z} = \sqrt{2}\bar{A}_0/\bar{A}_2$, and they are obtained from the relevant branching fractions as described above. The amplitudes of $I = 2$ are determined by the tree-level W boson exchange since the gluon penguin diagram has the nature of $\Delta I = 1/2$. In the SM, the $I = 2$ amplitudes are governed by the single weak phase of V_{ub}^L and thus there is no CP asymmetry in this channel except the small correction due to the electroweak penguin diagrams.

In the presence of the right-handed $b \rightarrow u$ current in Eq. (2), the amplitudes of $I = 2$ consist of the left- and right- handed contributions: $A_2 = A_{2L} + A_{2R}$ and $\bar{A}_2 = \bar{A}_{2L} + \bar{A}_{2R}$.

$C_{\pi^+\pi^-}$	-0.31 ± 0.05
$S_{\pi^+\pi^-}$	-0.66 ± 0.06
$C_{\pi^0\pi^0}$	-0.43 ± 0.24
$A_{CP}(B^+ \rightarrow \pi^+\pi^0)$	-0.026 ± 0.039
$\text{BR}(B \rightarrow \pi^+\pi^-)$	$(5.10 \pm 0.19) \times 10^{-6}$
$\text{BR}(B \rightarrow \pi^0\pi^0)$	$(1.91 \pm 0.225) \times 10^{-6}$
$\text{BR}(B^\pm \rightarrow \pi^\pm\pi^0)$	$(5.48 \pm 0.345) \times 10^{-6}$

TABLE I. Experimental data in $B \rightarrow \pi\pi$, taken from the compilation by HFAG [8].

Thus, the large imaginary part of V_{ub}^R/V_{ub}^L suggested by the analysis in Sec. II implies a possibility of CP violation in the $I = 2$ channel. We neglect the electroweak penguins in the following analysis because effects of the RHC are expected to be larger than them.

The direct CP asymmetry in $B^+ \rightarrow \pi^+\pi^0$, which vanishes in the SM, is written as

$$A_{CP}(B^+ \rightarrow \pi^+\pi^0) = \frac{1 - |R_{\pi\pi}|^2}{1 + |R_{\pi\pi}|^2}, \quad (26)$$

where the effect of the RHC in the $I = 2$ channel is represented by

$$R_{\pi\pi} \equiv \frac{1 + \bar{A}_{2R}/\bar{A}_{2L}}{1 + A_{2R}/A_{2L}}. \quad (27)$$

Other CPV observables are also affected by the RHC:

$$C_{\pi^+\pi^-} = \left(1 - |R_{\pi\pi}|^2 \left| \frac{1 + \bar{z}}{1 + z} \right|^2\right) / \left(1 + |R_{\pi\pi}|^2 \left| \frac{1 + \bar{z}}{1 + z} \right|^2\right), \quad (28)$$

$$S_{\pi^+\pi^-} = \sqrt{1 - C_{\pi^+\pi^-}^2} \sin \left(2\phi_2^L + \arg(R_{\pi\pi}) + \arg\left(\frac{1 + \bar{z}}{1 + z}\right)\right), \quad (29)$$

and

$$C_{\pi^0\pi^0} = \left(1 - |R_{\pi\pi}|^2 \left| \frac{2 - \bar{z}}{2 - z} \right|^2\right) / \left(1 + |R_{\pi\pi}|^2 \left| \frac{2 - \bar{z}}{2 - z} \right|^2\right), \quad (30)$$

where ϕ_2^L is one of the angles of the unitarity triangle in Fig. 1 and $C_{\pi^0\pi^0}$ is the counter part of $C_{\pi^+\pi^-}$ in $B \rightarrow \pi^0\pi^0$. We note that $C_{\pi^0\pi^0}$ is determined with the time-integrated decay rate of the tagged $B \rightarrow \pi^0\pi^0$ process. The experimental data of these observables and relevant CP averaged branching fractions are summarized in Table I. The phase ϕ_2^L is extracted from the unitarity triangle construction indicated in Fig. 1 as $\phi_2^L = 84.7^\circ \pm 7.5^\circ$.

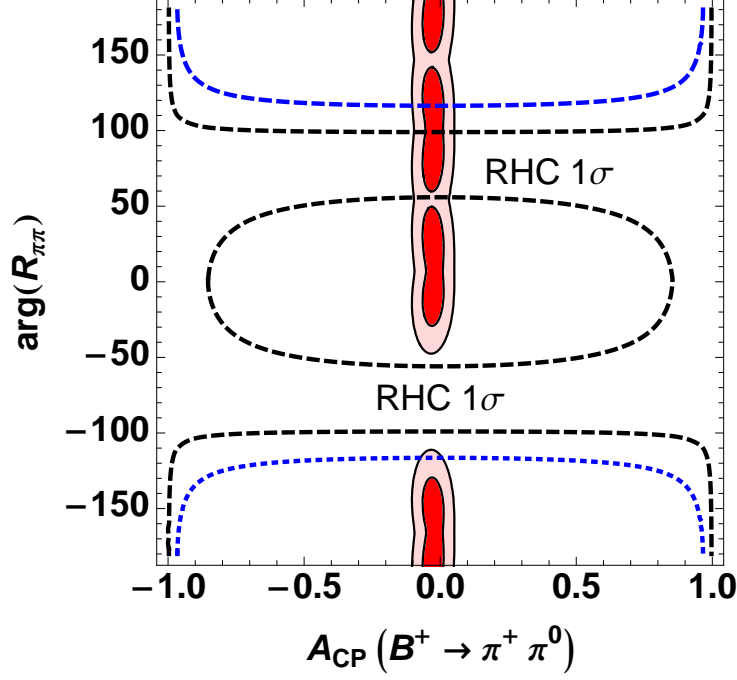


FIG. 3. Allowed region of the direct CP asymmetry and the phase discrepancy in $B \rightarrow \pi\pi$. The dark (light) red region is 1σ (2σ). The prediction of the CPV RHC is also shown: The region between the black dashed ellipse and two black dashed lines represents the 1σ prediction as indicated and the region between the blue dotted lines is 2σ .

We determine or constrain $R_{\pi\pi}$ with these data as shown in Fig. 3. The abscissa is the CP asymmetry $A_{CP}(B^+ \rightarrow \pi^+\pi^0)$, which is uniquely related to $|R_{\pi\pi}|$ as seen in Eq. (26), and the ordinate is $\arg(R_{\pi\pi})$, which represents the possible discrepancy in the ϕ_2 measurements between $B \rightarrow \pi\pi$ and the unitarity triangle as seen in Eq. (29). A strong constraint is given for $A_{CP}(B^+ \rightarrow \pi^+\pi^0)$, while $\arg(R_{\pi\pi})$ is restricted rather weakly because of the eight-fold ambiguity in the isospin analysis.

The dependence of $R_{\pi\pi}$ on V_{ub}^R is obtained by evaluating A_{2R}/A_{2L} in the factorization approximation:

$$\frac{A_{2R}}{A_{2L}} \simeq 1.56 \frac{V_{ub}^{R*}}{V_{ub}^{L*}} e^{i\delta_{\pi\pi}}, \quad (31)$$

where we introduce a strong phase $\delta_{\pi\pi}$ as an arbitrary parameter, which cannot be evaluated by the factorization method. A similar expression is obtained for $\bar{A}_{2R}/\bar{A}_{2L}$ replacing V_{ub}^{R*}/V_{ub}^{L*} by its complex conjugate. The details of the calculation using renormalization group equations (RGE) and the factorization is relegated in Appendix B 1.

In Fig. 3, taking the strong phase $\delta_{\pi\pi}$ as a free parameter, we also present the prediction on

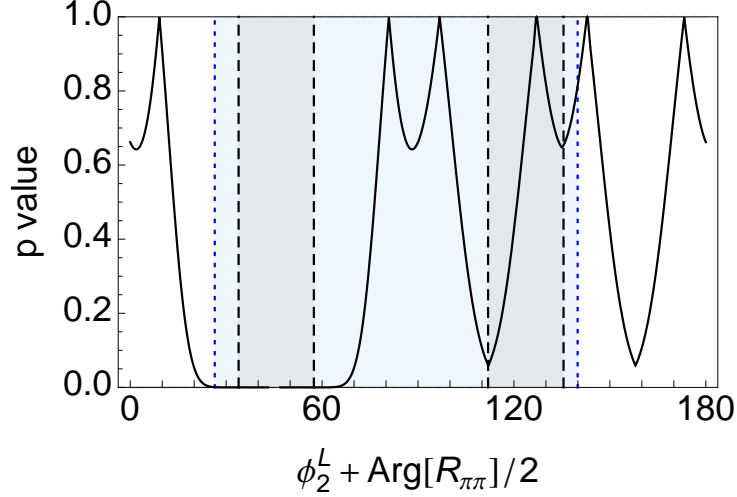


FIG. 4. The p value of $\phi_2^L + \arg(R_{\pi\pi})/2$ assuming $\sin \delta_{\pi\pi} = 0$ (solid line). The 1σ (2σ) prediction of the CPV RHC is also shown as the shaded region with vertical black dashed (blue dotted) boundaries.

$A_{CP}(B^+ \rightarrow \pi^+\pi^0)$ and $\arg(R_{\pi\pi})$ for the allowed range of V_{ub}^R/V_{ub}^L shown in Fig. 2. If V_{ub}^R/V_{ub}^L has a significant imaginary part as suggested in Sec. II, the almost vanishing $A_{CP}(B^+ \rightarrow \pi^+\pi^0)$ requires $\delta_{\pi\pi} \simeq 0$ or π , and $\arg(R_{\pi\pi})$ is sizable although its measurement suffers from the eight-fold ambiguity mentioned above. Figure 4 shows the p value of $\phi_2^L + \arg(R_{\pi\pi})/2$ assuming $\sin \delta_{\pi\pi} = 0$ as well as its range predicted for the allowed region of V_{ub}^R/V_{ub}^L in Fig. 2. The six-peak structure corresponds to the eight-fold ambiguity since each of the peaks at 127° and 143° consists of two solutions. The rather wide overlap between the theoretical prediction and the experimentally allowed region is partly due to the multifold ambiguity, and shows that both the SM and the scenario of the CPV RHC are consistent with the present $B \rightarrow \pi\pi$ data.

B. $B \rightarrow \rho\rho$

The isospin analysis can be applied to $B \rightarrow \rho\rho$ as in $B \rightarrow \pi\pi$ provided that the helicity state of the ρ mesons is identified by the angular analysis [20]. The possible final helicity states are $\rho_L\rho_L$ and $\rho_T\rho_T$, where $\rho_{L(T)}$ denotes the longitudinal (transverse) helicity state of ρ meson. The final state of $\rho_T\rho_T$ is a mixture of CP -even and CP -odd states, whereas $\rho_L\rho_L$ is purely CP -even as $\pi\pi$. Hence, we can study CP violation in $B \rightarrow \rho_L\rho_L$ in a similar manner

$C_{\rho_L^+ \rho_L^-}$	-0.06 ± 0.13
$S_{\rho_L^+ \rho_L^-}$	-0.05 ± 0.17
$C_{\rho_L^0 \rho_L^0}$	$0.2 \pm 0.8 \pm 0.3$
$S_{\rho_L^0 \rho_L^0}$	$0.3 \pm 0.7 \pm 0.2$
$A_{CP}(B^+ \rightarrow \rho_L^+ \rho_L^0)$	0.051 ± 0.054
$\text{BR}(B^\pm \rightarrow \rho^\pm \rho^0)$	$(24.0 \pm 1.95) \times 10^{-6}$
$\text{BR}(B \rightarrow \rho^+ \rho^-)$	$(24.2 \pm 3.15) \times 10^{-6}$
$\text{BR}(B \rightarrow \rho^0 \rho^0)$	$(0.73 \pm 0.275) \times 10^{-6}$
$f_L(B^\pm \rightarrow \rho^\pm \rho^0)$	0.950 ± 0.016 [22, 23]
$f_L(B \rightarrow \rho^+ \rho^-)$	0.977 ± 0.026 [24, 25]
$f_L(B \rightarrow \rho^0 \rho^0)$	0.618 ± 0.118 [22, 26]

TABLE II. Experimental data in $B \rightarrow \rho\rho$, taken from HFAG [8] unless otherwise indicated.

as $B \rightarrow \pi\pi$. We note that BABAR and Belle experiments have reported the dominance of the longitudinal final states in $B^+ \rightarrow \rho^+ \rho^0$ and $B \rightarrow \rho^+ \rho^-$. Although a 2.1σ difference between BABAR and Belle in the fraction of the longitudinal state in $B \rightarrow \rho^0 \rho^0$ exists [21], the longitudinal fraction is likely to be sizable. Accordingly, we focus on CP violation in $B \rightarrow \rho_L \rho_L$ in this work.

As in the above analysis of $B \rightarrow \pi\pi$, CPV observables $C_{\rho_L^+ \rho_L^-}$, $S_{\rho_L^+ \rho_L^-}$, $C_{\rho_L^0 \rho_L^0}$, $A_{CP}(B^+ \rightarrow \rho_L^+ \rho_L^0)$ are given in terms of z , \bar{z} , $R_{\rho_L \rho_L}$ and ϕ_2^L . In addition to these observables, the mixing-induced CP asymmetry in $B \rightarrow \rho_L^0 \rho_L^0$, denoted as $S_{\rho_L^0 \rho_L^0}$, is measurable and represented as

$$S_{\rho_L^0 \rho_L^0} = \sqrt{1 - C_{\rho_L^0 \rho_L^0}^2} \sin \left(2\phi_2^L + \arg(R_{\rho_L \rho_L}) + \arg \left(\frac{2 - \bar{z}}{2 - z} \right) \right). \quad (32)$$

We summarize the experimental values of the CPV parameters as well as the relevant branching and longitudinal fractions (f_L 's) in Table II.

These experimental data constrain $R_{\rho_L \rho_L}$ and the allowed region is presented in Fig. 5, in which $A_{CP}(B^+ \rightarrow \rho_L^+ \rho_L^0)$ and $\arg(R_{\rho_L \rho_L})$ are chosen as axes. It turns out that the triangle dictated by the isospin relation, $A(B^+ \rightarrow \rho_L^+ \rho_L^0) = A(B^0 \rightarrow \rho_L^+ \rho_L^-)/\sqrt{2} + A(B^0 \rightarrow \rho_L^0 \rho_L^0)$, and the charge-conjugated one are squashed. Hence, only a two-fold ambiguity remains in the isospin analysis in $B \rightarrow \rho_L \rho_L$ in contrast to the eight-fold one in $B \rightarrow \pi\pi$. This reduction of the number of solutions results in a more stringent restriction on $\arg(R_{\rho_L \rho_L})$ as seen in

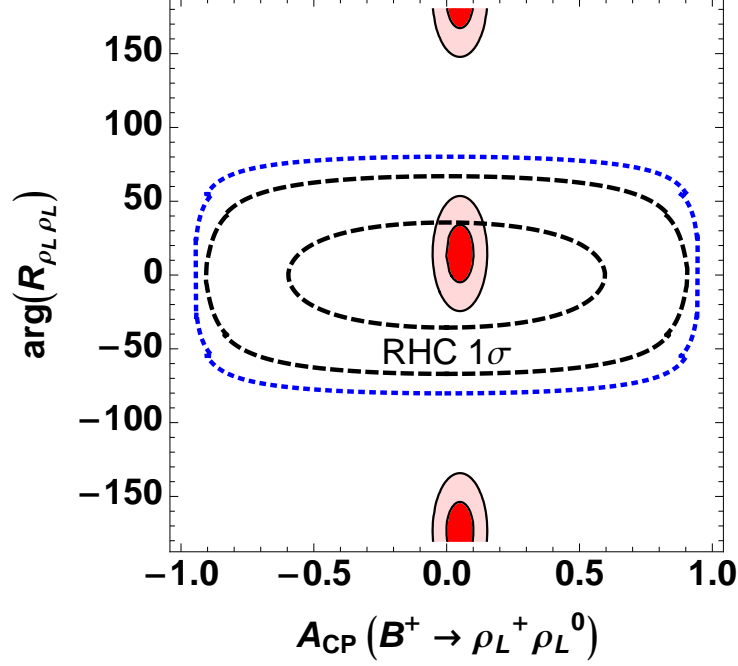


FIG. 5. Allowed region of the direct CP asymmetry and the possible phase discrepancy in $B \rightarrow \rho_L \rho_L$ is shown in the same manner as Fig. 3. The prediction of the CPV RHC is presented as well. The region between two black dashed ovals is 1σ and the region surrounded by the blue dotted one is 2σ .

Fig. 5. In other words, the possible discrepancy in the ϕ_2 determinations between $B \rightarrow \rho_L \rho_L$ and the unitarity triangle are constrained more strongly.

We evaluate $R_{\rho_L \rho_L}$ in the presence of the CPV RHC using the RGE and the factorization method as in the case of $B \rightarrow \pi\pi$. We obtain A_{2R}/A_{2L} as

$$\frac{A_{2R}}{A_{2L}} \simeq -0.91 \frac{V_{ub}^{R*}}{V_{ub}^{L*}} e^{i\delta_{\rho_L \rho_L}}, \quad (33)$$

where an independent strong phase $\delta_{\rho_L \rho_L}$ is introduced. This calculation is described in Appendix B 2. The predicted region of $R_{\rho_L \rho_L}$ for the allowed V_{ub}^R/V_{ub}^L shown in Fig. 2 and arbitrary values of $\delta_{\rho_L \rho_L}$ is also depicted in Fig. 5. One of the two experimentally allowed regions, which is consistent with the SM, is also compatible with the scenario of the CPV RHC. In Fig. 6, we present the p value of $\phi_2^L + \arg(R_{\rho_L \rho_L})/2$ assuming $\sin \delta_{\rho_L \rho_L} = 0$ as well as its range predicted for the allowed region of V_{ub}^R/V_{ub}^L in Fig. 2. The CPV RHC is consistent with one of the two possible solutions that is also favored in the SM. One may judge from Figs. 5 and 6 that the CPV RHC is incompatible with the experimental data at the 1σ level. However this is not the case because of the theoretical uncertainty in the factorization. We

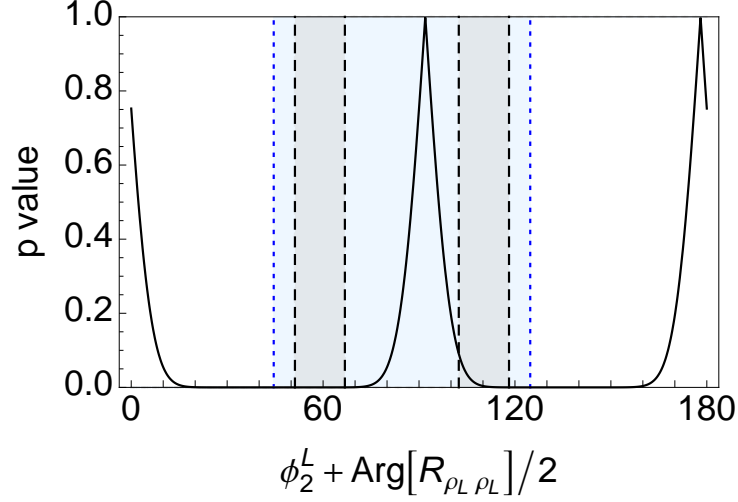


FIG. 6. The p value of $\phi_2^L + \arg(R_{\rho_L \rho_L})/2$ assuming $\sin \delta_{\rho_L \rho_L} = 0$ and the prediction of the CPV RHC as in Fig. 4.

consider that an uncertainty of a factor of two is likely.

C. $B \rightarrow DK$

Two quark processes $\bar{b} \rightarrow \bar{c}u\bar{s}$ and $\bar{b} \rightarrow \bar{u}c\bar{s}$ (and their charge conjugates) give rise to $B^\pm \rightarrow DK^\pm$ decays in the SM and the latter is modified by the $b \rightarrow u$ RHC. We denote the relevant decay amplitudes in the following manner:

$$A(B^+ \rightarrow \bar{D}^0 K^+) = A_B, \quad (34)$$

$$A(B^+ \rightarrow D^0 K^+) = A_B r_+ e^{i(\phi_{DK} + \delta_{DK})}, \quad (35)$$

$$A(B^- \rightarrow D^0 K^-) = A_B, \quad (36)$$

$$A(B^- \rightarrow \bar{D}^0 K^-) = A_B r_- e^{i(-\phi_{DK} + \delta_{DK})}, \quad (37)$$

where amplitude ratios r_\pm are defined to be positive. This decay mode is employed to extract $\phi_3^L = \arg(V_{ub}^{L*})$ (or γ) of the unitarity triangle in the SM [27–29], in which the right-handed contribution vanishes and $\phi_{DK} = \phi_3^L$. We stress that $r_+ = r_-$ in the SM, but this is not the case in the presence of the CPV RHC in general. Thus a direct CP asymmetry,

$$A_{CP}(B^+ \rightarrow D^0 K^+) = \frac{\Gamma(B^+ \rightarrow D^0 K^+) - \Gamma(B^- \rightarrow \bar{D}^0 K^-)}{\Gamma(B^+ \rightarrow D^0 K^+) + \Gamma(B^- \rightarrow \bar{D}^0 K^-)} = \frac{r_+^2 - r_-^2}{r_+^2 + r_-^2}, \quad (38)$$

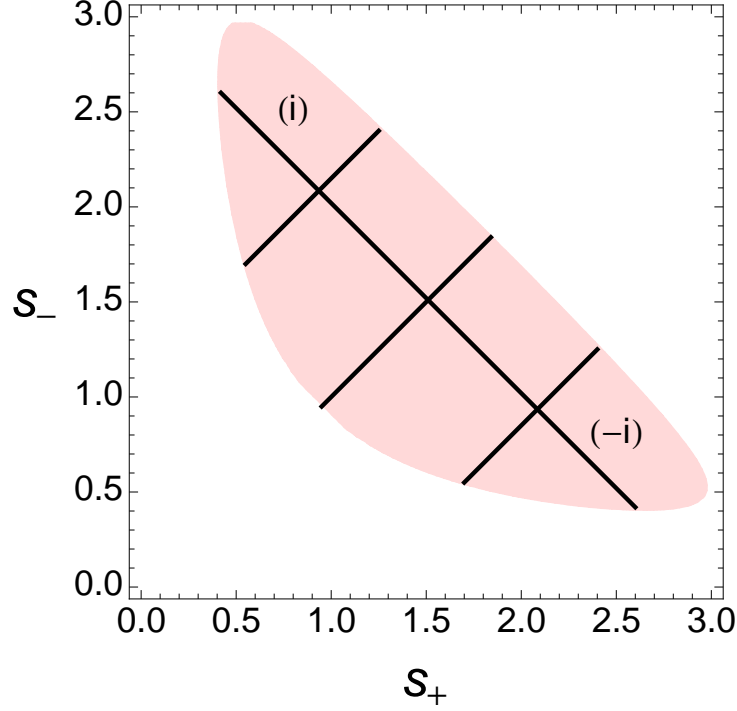


FIG. 7. An illustration of the binning in the Dalitz plot method.

is induced in addition to a discrepancy between ϕ_{DK} and ϕ_3^L . Among several methods to extract ϕ_3 in the SM, we focus on the most powerful one, that is the Dalitz plot method [29], in which the neutral D meson in $B^\pm \rightarrow DK^\pm$ is identified with its Dalitz decay $D \rightarrow K_S \pi^+ \pi^-$. We extend the method to the case of $r_+ \neq r_-$ in the following.

Amplitudes of the Dalitz decay are written as

$$A(D^0 \rightarrow K_S(p_K) \pi^+(p_+) \pi^-(p_-)) = A_D(s_+, s_-), \quad (39)$$

$$A(\bar{D}^0 \rightarrow K_S(p_K) \pi^+(p_+) \pi^-(p_-)) = A_D(s_-, s_+), \quad (40)$$

where $s_+ = (p_K + p_+)^2$ and $s_- = (p_K + p_-)^2$. We neglect small meson-antimeson mixing and CP violation in the neutral D meson system in the present work. Then, the differential decay rate of $B^\pm \rightarrow (K_S \pi^+ \pi^-)_D K^\pm$ is represented as

$$\begin{aligned} d\Gamma(B^\pm \rightarrow (K_S \pi^+ \pi^-)_D K^\pm) \\ = |A_B|^2 \left[|A_D(s_\mp, s_\pm)|^2 + r_\pm^2 |A_D(s_\pm, s_\mp)|^2 + 2r_\pm \text{Re} \left\{ e^{i(\pm\phi_{DK} + \delta_{DK})} A_D^*(s_\mp, s_\pm) A_D(s_\pm, s_\mp) \right\} \right] d\Phi, \end{aligned} \quad (41)$$

where $d\Phi$ is a phase-space factor.

In the Dalitz plot method, the phase space is divided into $2k$ bins as illustrated in Fig. 7. The binning is symmetric with respect to the diagonal line defined by $s_+ = s_-$, and the i -th bin ($i = 1, 2, \dots, k$) with $s_+ < s_-$ and the $(-i)$ -th bin with $s_+ > s_-$ form a symmetric pair. The partial decay rate into the i -th bin is written as

$$\begin{aligned}\Gamma_i^\pm &= \int_i d\Gamma(B^\pm \rightarrow (K_S \pi^+ \pi^-)_D K^\pm) \\ &= |A_B|^2 \left[T_{\mp i} + r_\pm^2 T_{\pm i} + 2r_\pm \sqrt{T_i T_{-i}} \{c_i \cos(\pm\phi_{DK} + \delta_{DK}) \mp s_i \sin(\pm\phi_{DK} + \delta_{DK})\} \right], \quad (42)\end{aligned}$$

and that into the $(-i)$ -th bin is

$$\begin{aligned}\Gamma_{-i}^\pm &= \int_{-i} d\Gamma(B^\pm \rightarrow (K_S \pi^+ \pi^-)_D K^\pm) \\ &= |A_B|^2 \left[T_{\pm i} + r_\pm^2 T_{\mp i} + 2r_\pm \sqrt{T_i T_{-i}} \{c_i \cos(\pm\phi_{DK} + \delta_{DK}) \pm s_i \sin(\pm\phi_{DK} + \delta_{DK})\} \right], \quad (43)\end{aligned}$$

where

$$T_{\pm i} = \int_{\pm i} d\Phi |A_D(s_+, s_-)|^2, \quad (44)$$

$$c_{\pm i} = \int_{\pm i} d\Phi \operatorname{Re}[A_D(s_+, s_-) A_D^*(s_-, s_+)] / \sqrt{T_i T_{-i}}, \quad (45)$$

$$s_{\pm i} = \int_{\pm i} d\Phi \operatorname{Im}[A_D(s_+, s_-) A_D^*(s_-, s_+)] / \sqrt{T_i T_{-i}}, \quad (46)$$

and we have used $c_i = c_{-i}$ and $s_i = -s_{-i}$.

The Dalitz distribution $|A_D(s_+, s_-)|^2$ is given by the flavor-tagged neutral D meson decay and thus $T_{\pm i}$'s are known as well as $|A_B|^2$, which is determined by the flavor specific D decay in $B^\pm \rightarrow DK^\pm$. We notice that the number of unknown quantities ($c_i, s_i, r_\pm, \phi_{DK}$ and δ_{DK}) is $2k + 4$, that of observables ($\Gamma_{\pm i}^\pm$) is $4k$, and in principle, all the unknown quantities can be determined provided $k \geq 2$. In particular, we can obtain the direct CP asymmetry in Eq. (38) and the angle discrepancy $\phi_{DK} - \phi_3^L$ with the (extended) Dalitz plot method.

It is possible to improve the analysis by using c_i 's and s_i 's independently extracted from data at a charm factory [29]. The entangled $D^0 \bar{D}^0$ states produced near the threshold exhibit quantum interference that depends on c_i 's and s_i 's.

In Ref. [30], experimental data of Belle corresponding to $\Gamma_{\pm i}^\pm, T_{\pm i}$ are shown for the optimized binning [31] with $k = 8$. The result for c_i 's and s_i 's by CLEO collaboration [32] is also summarized in Ref. [30]. Using these data, we obtain a constraint on the direct CP asymmetry $A_{CP}(B^+ \rightarrow D^0 K^+)$ and the phase disagreement $\arg(R_{DK}) (= -2(\phi_{DK} - \phi_3^L))$, see

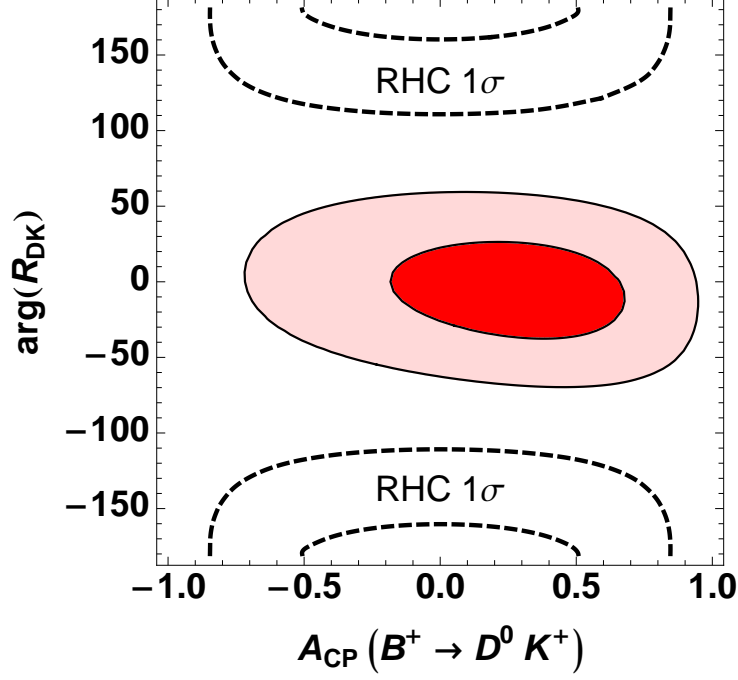


FIG. 8. Allowed region of the direct CP asymmetry and the possible phase discrepancy in $B \rightarrow DK$ as in the same manner in Fig. 3. The prediction of the CPV RHC is also shown. The region between two black dashed ellipses is 1σ prediction as denoted and the whole plane is practically allowed at the 2σ level.

Eq. (52) below.) as presented in Fig. 8. Although the restriction is rather mild at present, we confirm that the extended Dalitz plot method does work and expect a better sensitivity in future.

In order for a comparison with the allowed region in Fig. 8, we evaluate the effect of the CPV RHC on $B^+ \rightarrow D^0 K^+$ and the charge conjugation mode. Their amplitudes are decomposed into the left- and right- handed contributions:

$$A(B^+ \rightarrow D^0 K^+) = |A_L|e^{i(\phi_3^L + \delta_L)} + |A_R|e^{i(\phi_3^R + \delta_R)}, \quad (47)$$

and

$$A(B^- \rightarrow \bar{D}^0 K^-) = |A_L|e^{i(-\phi_3^L + \delta_L)} + |A_R|e^{i(-\phi_3^R + \delta_R)}, \quad (48)$$

where $\phi_3^{L(R)} = \arg(V_{ub}^{L(R)*})$ is the weak phase of the left(right)-handed current and $\delta_{L,R}$

denote strong phases. It is convenient to introduce an amplitude ratio as

$$R_{DK} = e^{2i\phi_3^L} \frac{A(B^- \rightarrow \bar{D}^0 K^-)}{A(B^+ \rightarrow D^0 K^+)} \quad (49)$$

$$= \frac{1 + |A_R/A_L| e^{i(-\phi_3^R + \phi_3^L + \delta)}}{1 + |A_R/A_L| e^{i(\phi_3^R - \phi_3^L + \delta)}} , \quad (50)$$

where $\delta = \delta_R - \delta_L$. Then, it is straightforward to obtain the following relations from Eqs. (35), (37) and (38):

$$A_{CP}(B^+ \rightarrow D^0 K^+) = \frac{1 - |R_{DK}|^2}{1 + |R_{DK}|^2} , \quad (51)$$

and

$$\phi_{DK} = \phi_3^L - \arg(R_{DK})/2 . \quad (52)$$

The RGE and the factorization approximation gives

$$|A_R/A_L| = 4.99 |V_{ub}^R/V_{ub}^L| , \quad (53)$$

as described in Appendix B3.

We evaluate R_{DK} in Eq. (50) for the allowed value of V_{ub}^R/V_{ub}^L shown in Fig. 2 and ϕ_3^L determined by the unitarity triangle taking δ as a free parameter. Then, we obtain theoretical prediction on $A_{CP}(B^+ \rightarrow D^0 K^+)$ and $\arg(R_{DK})$ as presented in Fig. 8. We find that the scenario of the CPV RHC is disfavored at the 1σ level despite the moderate current experimental constraint though it is not excluded at 2σ . This is due to the enhancement of the RHC contribution in the DK mode shown in Eq. (53) compared to those in the $\pi\pi$ and $\rho_L\rho_L$ modes in Eqs. (31) and (33). This notable sensitivity, though it is derived in the factorization approximation, might play an important role in future experiments in order to probe or exclude the CPV RHC.

D. Prediction of the MSSM

It has been pointed out that the $b \rightarrow u$ RHC is induced by radiative corrections in the MSSM [4, 33]. The gluino-squark one-loop diagram with simultaneous insertions of the left-right mixing in the (3,3) component of the down-type squark mass matrix (Δ_{33}^{dLR}) and that in the (1,3) component of the up-type squark mass matrix (Δ_{13}^{uRL}) gives the dominant contribution and one obtains

$$V_{ub}^R = \frac{\alpha_s}{36\pi} \delta_{33}^{dLR} \delta_{13}^{uRL} , \quad (54)$$

where the dimensionless mass insertion parameters are defined by $\delta_{33}^{dLR} = \Delta_{33}^{dLR}/M_{\text{SUSY}}^2$ and $\delta_{13}^{uRL} = \Delta_{13}^{uRL}/M_{\text{SUSY}}^2$, and the masses of relevant supersymmetric partners are assumed to be common for simplicity and denoted by M_{SUSY} .

In Fig. 2, we present V_{ub}^R/V_{ub}^L evaluated with V_{ub}^L in Eq. (16) and V_{ub}^R in Eq. (54) for $|\delta_{33}^{dLR}\delta_{13}^{uRL}| = 0.1$ and 0.3 . We observe that the MSSM contribution is consistent with the current experimental bound from $|V_{ub}|$ determination and the unitarity triangle within 2σ though the best fitted values do not seem to be realized. A future experiment like SuperKEKB/Belle II may find a signal of supersymmetry through the $b \rightarrow u$ RHC.

IV. CONCLUSION

We have studied the scenario of $b \rightarrow u$ right-handed current. Our analysis combining the present experimental results for direct $|V_{ub}|$ determination with the unitarity triangle suggests a significant CPV RHC in the $b \rightarrow u$ transition as presented in Fig. 2.

According to this analysis, we have examined CPV signals in two-body hadronic B decays: $B \rightarrow \pi\pi$, $B \rightarrow \rho\rho$ and $B \rightarrow DK$. The expected signals in these decay modes are new direct CP asymmetries, deviations of ϕ_2 in $B \rightarrow \pi\pi, \rho\rho$ and that of ϕ_3 in $B \rightarrow DK$; they are depicted in Figs. 3, 5 and 8 as well as the present experimental constraints. Although the direct CP asymmetries in $B \rightarrow \pi\pi, \rho\rho$ are strongly constrained, a sizable deviation of $\sim 50^\circ$ in ϕ_2 is not excluded. As for $B \rightarrow DK$, the effect of RHC is enhanced by QCD radiative correction in the factorization approximation. Hence the rather moderate current experimental bound tightly restricts the CPV RHC. We have found that the consistency of the suggested CPV RHC with the present $B \rightarrow DK$ data is in between the 1σ and 2σ levels in the factorization approximation. The prediction of the MSSM is also compared to the allowed region of V_{ub}^R/V_{ub}^L as shown in Fig. 2.

In conclusion, the $b \rightarrow u$ right-handed current is a new physics scenario that is still consistent with the present experimental data. The suggested large CP violation gives rise to the new CP violating signals in hadronic B decays and they may be detected in a future B factory experiment.

ACKNOWLEDGMENTS

We thank R. Watanabe for discussion in the initial stage of this study. The work of MT is supported in part by JSPS KAKENHI Grant Number 25400257.

Appendix A: Hadronic form factors in $B \rightarrow (\pi, \rho, \omega)\ell\bar{\nu}$

We briefly summarize the hadronic form factors used in our numerical analysis in the main text.

1. $B \rightarrow \pi$

The hadronic form factor $f_+(q^2)$ in Eq. (6) is defined as

$$\langle \pi | \bar{u} \gamma^\mu b | \bar{B} \rangle = f_+(q^2)(p_B^\mu + p_\pi^\mu) + f_-(q^2)q^\mu. \quad (\text{A1})$$

The result of LCSR is concisely parameterized in the following form of pole dominance [10]:

$$f_+(q^2) = \frac{r_1}{1 - q^2/m_1^2} + \frac{r_2}{1 - q^2/m_{\text{fit}}^2}, \quad (\text{A2})$$

where $r_1 = 0.744$, $m_1^\pi = 5.32$ GeV, $r_2 = -0.486$ and $m_{\text{fit}}^2 = 40.73$ GeV².

2. $B \rightarrow \rho, \omega$

The form factors in Eqs. (9) and (10) are parameterized as

$$A_1(q^2) = \frac{r_1^{A_1}}{1 - q^2/m_{\text{fit}}^{A_1^2}}, \quad (\text{A3})$$

$$A_2(q^2) = \frac{r_1^{A_2}}{1 - q^2/m_{\text{fit}}^{A_2^2}} + \frac{r_2^{A_2}}{(1 - q^2/m_{\text{fit}}^{A_2^2})^2}, \quad (\text{A4})$$

and

$$V(q^2) = \frac{r_1^V}{1 - q^2/m_{1^-}^2} + \frac{r_2^V}{1 - q^2/m_{\text{fit}}^{V^2}}. \quad (\text{A5})$$

The LCSR gives [11] $r_1^{A_1} = 0.240$, $m_{\text{fit}}^{A_1^2} = 37.51\text{GeV}^2$, $r_1^{A_2} = 0.009$, $r_2^{A_2} = 0.212$, $m_{\text{fit}}^{A_2^2} = 40.82\text{GeV}^2$, $r_1^V = 1.045$, $r_2^V = -0.721$, $m_{1^-} = 5.32\text{GeV}$, $m_{\text{fit}}^{V^2} = 38.34\text{GeV}^2$ for $B \rightarrow \rho$, and $r_1^{A_1} = 0.217$, $m_{\text{fit}}^{A_1^2} = 37.01\text{GeV}^2$, $r_1^{A_2} = 0.006$, $r_2^{A_2} = 0.192$, $m_{\text{fit}}^{A_2^2} = 41.24\text{GeV}^2$, $r_1^V = 1.006$, $r_2^V = -0.713$, $m_{1^-} = 5.32\text{GeV}$, $m_{\text{fit}}^{V^2} = 37.45\text{GeV}^2$ for $B \rightarrow \omega$.

Appendix B: Evaluation of amplitudes by the factorization

In this Appendix, we describe the calculation of $B \rightarrow \pi\pi, \rho\rho, DK$ amplitudes in the factorization method.

1. $B \rightarrow \pi\pi$

The effective four-fermion hamiltonian that contributes to the $I = 2$ channel in $B \rightarrow \pi\pi$ is decomposed into the left and right pieces as $\mathcal{H}_{\text{eff}} = \mathcal{H}_L + \mathcal{H}_R$, and

$$\mathcal{H}_X = 2\sqrt{2}G_F V_{ud}V_{ub}^{X*} [C_{1X}(\mu)O_{1X}(\mu) + C_{2X}(\mu)O_{2X}(\mu)] + \text{h.c.}, \quad (\text{B1})$$

where $X = L, R$ and μ denotes a renormalization scale. The four-fermion operators are defined by

$$O_{1X} = \bar{u}_L^\alpha \gamma^\nu d_L^\beta \bar{b}_X^\beta \gamma_\nu u_X^\alpha, \quad (\text{B2})$$

$$O_{2X} = \bar{u}_L^\alpha \gamma^\nu d_L^\alpha \bar{b}_X^\beta \gamma_\nu u_X^\beta, \quad (\text{B3})$$

where α and β are color indices. Wilson coefficients C_{jX} ($j = 1, 2$) are obtained by solving a set of renormalization group equations in the leading order [34]. The relevant anomalous dimensions are

$$\gamma_L = \frac{\alpha_s}{4\pi} \begin{pmatrix} -2 & 6 \\ 6 & -2 \end{pmatrix}, \quad \gamma_R = \frac{\alpha_s}{4\pi} \begin{pmatrix} -16 & 0 \\ -6 & 2 \end{pmatrix}, \quad (\text{B4})$$

for O_{jL} and O_{jR} respectively. As a result, we obtain the Wilson coefficients at the bottom quark mass scale (m_b):

$$C_{1L}(m_b) = \frac{1}{2} \left(\left[\frac{\alpha_s(m_b)}{\alpha_s(m_W)} \right]^{-6/23} - \left[\frac{\alpha_s(m_b)}{\alpha_s(m_W)} \right]^{12/23} \right) \simeq -0.27, \quad (\text{B5})$$

$$C_{2L}(m_b) = \frac{1}{2} \left\{ \left[\frac{\alpha_s(m_b)}{\alpha_s(m_W)} \right]^{-6/23} + \left[\frac{\alpha_s(m_b)}{\alpha_s(m_W)} \right]^{12/23} \right\} \simeq 1.12, \quad (\text{B6})$$

$$C_{1R}(m_b) = \frac{1}{3} \left\{ \left[\frac{\alpha_s(m_b)}{\alpha_s(m_W)} \right]^{24/23} - \left[\frac{\alpha_s(m_b)}{\alpha_s(m_W)} \right]^{-3/23} \right\} \simeq 0.34, \quad (\text{B7})$$

and

$$C_{2R}(m_b) = \left[\frac{\alpha_s(m_b)}{\alpha_s(m_W)} \right]^{-3/23} \simeq 0.92, \quad (\text{B8})$$

where $\alpha_s(m_Z) = 0.118$ [16] and $m_b = 4.2$ GeV [35] are used. We neglect the gluon penguin operators since they do not contribute to the $I = 2$ final state.

The amplitude ratio A_{2R}/A_{2L} is conveniently evaluated by calculating $B^+ \rightarrow \pi^+\pi^0$ amplitudes, $\langle \pi^+\pi^0 | \mathcal{H}_X | B^+ \rangle$, at $\mu = m_b$:

$$\begin{aligned} \langle \pi^+\pi^0 | \mathcal{H}_L | B^+ \rangle &\simeq \frac{G_F}{\sqrt{2}} V_{ud} V_{ub}^{L*} \left[\{C_{1L}(m_b) + C_{2L}(m_b)/3\} \langle \pi^0 | \bar{u} \gamma^\nu \gamma_5 u | 0 \rangle \langle \pi^+ | \bar{b} \gamma_\nu d | B^+ \rangle \right. \\ &\quad \left. + \{C_{2L}(m_b) + C_{1L}(m_b)/3\} \langle \pi^+ | \bar{u} \gamma^\nu \gamma_5 d | 0 \rangle \langle \pi^0 | \bar{b} \gamma_\nu u | B^+ \rangle \right], \end{aligned} \quad (\text{B9})$$

and

$$\begin{aligned} \langle \pi^+\pi^0 | \mathcal{H}_R | B^+ \rangle &\simeq \frac{G_F}{\sqrt{2}} V_{ud} V_{ub}^{R*} \left[2\{C_{1R}(m_b) + C_{2R}(m_b)/3\} \langle \pi^0 | \bar{u} \gamma_5 u | 0 \rangle \langle \pi^+ | \bar{b} d | B^+ \rangle \right. \\ &\quad \left. + \{C_{2R}(m_b) + C_{1R}(m_b)/3\} \langle \pi^+ | \bar{u} \gamma^\nu \gamma_5 d | 0 \rangle \langle \pi^0 | \bar{b} \gamma_\nu u | B^+ \rangle \right], \end{aligned} \quad (\text{B10})$$

where we have used Fierz rearrangement and ignored annihilation terms and nonfactorizable contributions. The matrix elements of the vector currents in Eqs. (B9) and (B10) are expressed by the form factors in Eq. (A1) and those of the axial-vector currents are given by the pion decay constant. The (pseudo)scalar operator in Eq. (B10) are related to the corresponding (axial-)vector operator using the equation of motion of the quark fields and thus its matrix element is also written in terms of the form factors (the decay constant). Interestingly, we do not need to specify the values of the form factors and the decay constant since they disappear in the ratio $\langle \pi^+\pi^0 | \mathcal{H}_R | B^+ \rangle / \langle \pi^+\pi^0 | \mathcal{H}_L | B^+ \rangle$. Hence we obtain

$$\begin{aligned} \frac{A_{2R}}{A_{2L}} &= \frac{\langle \pi^+\pi^0 | \mathcal{H}_R | B^+ \rangle}{\langle \pi^+\pi^0 | \mathcal{H}_L | B^+ \rangle} \\ &\simeq \frac{V_{ub}^{R*}}{V_{ub}^{L*}} \frac{3}{4} \left[\frac{C_{2R}(m_b) + C_{1R}(m_b)/3}{C_{2L}(m_b) + C_{1L}(m_b)} + \frac{C_{1R}(m_b) + C_{2R}(m_b)/3}{C_{2L}(m_b) + C_{1L}(m_b)} \frac{m_\pi^2}{m_q M_b} \right] \simeq 1.56 \frac{V_{ub}^{R*}}{V_{ub}^{L*}}, \end{aligned} \quad (\text{B11})$$

where M_b denotes the bottom quark pole mass, m_q represents the average current mass of the up and down quarks, and we employ $M_b = 4.91$ GeV [35] and $m_q = 3.5$ MeV [16] in our numerical calculation.

The factorization method described above should be understood as a crude approximation that provides an order of magnitude. We consider that an uncertainty of a factor of two remains even in the ratio in Eq. (B11). Furthermore it gives no information on the phase shift by the strong interaction, and thus we introduce a strong phase in Eq. (31) by hand.

2. $B \rightarrow \rho\rho$

The effective four-fermion hamiltonian for $B \rightarrow \pi\pi$, shown in Eqs. (B1), (B2) and (B3), also describes the $I = 2$ amplitudes in $B \rightarrow \rho_L \rho_L$. The relevant matrix elements are

evaluated almost in the same way as in the case of $B \rightarrow \pi\pi$. We finally obtain

$$\frac{A_{2R}}{A_{2L}} = \frac{\langle \rho_L^+ \rho_L^0 | \mathcal{H}_R | B^+ \rangle}{\langle \rho_L^+ \rho_L^0 | \mathcal{H}_L | B^+ \rangle} = -\frac{V_{ub}^{R*}}{V_{ub}^{L*}} \frac{3}{4} \frac{C_{2R}(m_b) + C_{1R}(m_b)/3}{C_{2L}(m_b) + C_{1L}(m_b)} \simeq -0.91 \frac{V_{ub}^{R*}}{V_{ub}^{L*}}. \quad (\text{B12})$$

3. $B \rightarrow DK$

The effective hamiltonian for $B^+ \rightarrow D^0 K^+$ and its charge conjugation is given by $\mathcal{H}_{\text{eff}} = \mathcal{H}_L + \mathcal{H}_R$ and

$$\mathcal{H}_X = 2\sqrt{2}G_F V_{cs} V_{ub}^{X*} [C_{1X}(\mu) O_{1X}(\mu) + C_{2X}(\mu) O_{2X}(\mu)] + \text{h.c.}, \quad (\text{B13})$$

where the four-fermion operators are defined by

$$O_{1X} = \bar{c}_L^\alpha \gamma^\nu s_L^\beta \bar{b}_X^\beta \gamma_\nu u_X^\alpha, \quad (\text{B14})$$

$$O_{2X} = \bar{c}_L^\alpha \gamma^\nu s_L^\alpha \bar{b}_X^\beta \gamma_\nu u_X^\beta. \quad (\text{B15})$$

The renormalization of these operators are the same as those in $B \rightarrow \pi\pi$ in the leading order and hence the Wilson coefficients are also given by Eqs. (B5), (B6), (B7) and (B8).

Using Fierz rearrangement and ignoring annihilation terms and nonfactorizable contributions, we evaluate the amplitude ratio A_R/A_L as in the case of $B \rightarrow \pi\pi$. Eventually, we obtain

$$\left| \frac{A_R}{A_L} \right| = \left| \frac{V_{ub}^{R*}}{V_{ub}^{L*}} \right| \frac{2m_D^2}{M_b M_c} \frac{C_{2R}(m_b) + 3C_{1R}(m_b)}{C_{2L}(m_b) + 3C_{1L}(m_b)} \simeq 4.99 \left| \frac{V_{ub}^{R*}}{V_{ub}^{L*}} \right|, \quad (\text{B16})$$

where $M_c = 1.77$ GeV denotes the charm quark pole mass [35] and we have neglected the up and strange quark masses. The quark pole masses emerge when we utilize the equations of motion of the quark fields in order to evaluate the contribution of the RHC. We note that the $B \rightarrow K$ form factors and the D meson decay constant appearing in each amplitude A_X cancel out in the ratio of Eq. (B16) as in $B \rightarrow \pi\pi$.

-
- [1] N. Cabibbo, Phys. Rev. Lett. **10**, 531 (1963).
 - [2] M. Kobayashi and T. Maskawa, Prog. Theor. Phys. **49**, 652 (1973).
 - [3] C. -H. Chen and S. -H. Nam, Phys. Lett. **B666**, 462 (2008).
 - [4] A. Crivellin, Phys. Rev. D **81**, 031301(R) (2010).
 - [5] A. Buras, K. Gemmler, G. Ishidori, Nucl. Phys. **B843**, 107 (2011).

- [6] I. Adachi *et al.* (Belle Collaboration), Phys. Rev. Lett. **110**, 131801 (2013). arXiv:1208.4678 [hep-ex].
- [7] A question whether new physics resolves the discrepancies among $|V_{ub}|$ (and $|V_{cb}|$) determinations is studied in the following paper: A. Crivellin and S. Pokorski, arXiv:1407.1320 [hep-ph].
- [8] Y. Amhis *et al.* (Heavy Flavor Averaging Group), arXiv:1207.1158 [hep-ex]. See also online update at <http://www.slac.stanford.edu/xorg/hfag/>.
- [9] Flavor Lattice Averaging Group, <http://itpwiki.unibe.ch/flag/>, 2013.
- [10] P. Ball and R. Zwicky, Phys. Rev. D **71**, 014015 (2005).
- [11] P. Ball and R. Zwicky, Phys. Rev. D **71**, 014029 (2005).
- [12] A. Sibidanov *et al.* (Belle Collaboration), Phys. Rev. D **88**, 032005 (2013).
- [13] F.U. Bernlochner, Z. Ligeti and S. Turczyk, arXiv:1408.2516 [hep-ph].
- [14] P. Gambino, P. Giordano, G. Ossola and N. Uraltsev, J. High Energy Phys. 10 (2007) 058.
- [15] L. Wolfenstein, Phys. Rev. Lett. 51, 1945 (1983).
- [16] K.A. Olive *et al.* (Particle Data Group), Chin. Phys. C, **38**, 090001 (2014). See also <http://pdg.lbl.gov/>.
- [17] CKMfitter Group (J. Charles *et al.*), Eur. Phys. J. C **41**, 1 (2005). For updated results, see <http://ckmfitter.in2p3.fr>.
- [18] For details see, for example, I. I. Bigi and A. I. Sanda, *CP Violation* (Second Edition), Cambridge University Press, Cambridge, UK (2009).
- [19] M. Gronau and D. London, Phys. Rev. Lett. **65**, 3381 (1990).
- [20] I. Dunietz, H. Quinn, A. Snyder, W. Toki and H. J. Lipkin, Phys. Rev. D. **43**, 2193 (1991).
- [21] P. Vanhoefer *et al.* (Belle Collaboration), Phys. Rev. D **89**, 072008 (2014).
- [22] J. Zhang *et al.* (Belle Collaboration), Phys. Rev. Lett. **91**, 221801 (2003).
- [23] B. Aubert *et al.* (BABAR Collaboration), Phys. Rev. Lett. **102**, 141802 (2009).
- [24] A. Somov *et al.* (Belle Collaboration), Phys. Rev. Lett. **96**, 171801 (2006).
- [25] B. Aubert *et al.* (BABAR Collaboration), Phys. Rev. D **76**, 052007 (2007).
- [26] B. Aubert *et al.* (BABAR Collaboration), Phys. Rev. D **78**, 071104(R) (2008).
- [27] M. Gronau and D. Wyler, Phys. Lett. **B265**, 172 (1991);
- [28] D. Atwood, I. Dunietz and A. Soni, Phys. Rev. Lett. **78**, 3257 (1997).
- [29] A. Giri, Y. Grossman, A. Soffer and J. Zupan, Phys. Rev. D **68**, 054018 (2003).
- [30] H. Aihara *et al.* (Belle Collaboration), Phys. Rev. D **85**, 112014 (2012).

- [31] A. Bondar and A. Poluektov, Eur. Phys. J. C **55**, 51 (2008).
- [32] J. Libby *et al.* (CLEO Collaboration), Phys. Rev. D **82**, 112006 (2010).
- [33] A. Crivellin and U. Nierste, Phys. Rev. D **79**, 035018 (2009).
- [34] See, for example, R.D.C. Miller and B.H.J. McKellar, Phys. Rep. **106**, 169 (1984); G. Buchalla, A.J. Buras and M.E. Lautenbacher, Rev. Mod. Phys. **68**, 1125 (1996).
- [35] Z.Z. Xing, H. Zhang and S. Zhou, Phys. Rev. D **77**, 113016, 2008. arXiv:0712.1419 [hep-ph].